JPE 19-1-22

https://doi.org/10.6113/JPE.2019.19.1.234
ISSN(Print): 1598-2092 / ISSN(Online): 2093-4718

Unbalanced Power Sharing for Islanded Droop-Controlled Microgrids

Yaoqin Jia†, Daoyang Li*, and Zhen Chen**

†,**State Key Laboratory of Electrical Insulation and Power Equipment,
Xi'an Jiaotong University, Xi'an, China
*Xuji Group Corporation, Xuchang, China

Abstract

Studying the control strategy of a microgrid under the load unbalanced state helps to improve the stability of the system. The magnitude of the power fluctuation, which occurs between the power supply and the load, is generated in a microgrid under the load unbalanced state is called negative sequence reactive power Q^-. Traditional power distribution methods such as P-f, Q-E droop control can only distribute power with positive sequence current information. However, they have no effect on Q^- with negative sequence current information. In this paper, a stationary-frame control method for power sharing and voltage unbalance compensation in islanded microgrids is proposed. This method is based on the proper output impedance control of distributed generation unit (DG unit) interface converters. The control system of a DG unit mainly consists of an active-power-frequency and reactive-power-voltage droop controller, an output impedance controller, and voltage and current controllers. The proposed method allows for the sharing of imbalance current among the DG unit and it can compensate voltage unbalance at the same time. The design approach of the control system is discussed in detail. Simulation and experimental results are presented. These results demonstrate that the proposed method is effective in the compensation of voltage unbalance and the power distribution.

Key words: Distributed generators, Microgrid, Power sharing, Voltage unbalance compensation

I. INTRODUCTION

The microgrid is emerging as a new way to integrate distributed generation units (DG units), which can provide more reliable electric service and higher power quality to customers [1]. Three-phase DC-AC inverters are usually used as the power electronic interface to connect a DG unit and a microgrid, through which the flexibility and reliability of the microgrid can be obtained. In addition, parallel inverter operation is a key issue that should be addressed. The control objective is to obtain power sharing in proportion to the rated capacity of the DG unit and to maintain good power qualities such as a good voltage waveform, amplitude and frequency.

Inverters are usually controlled as voltage sources to provide voltage support. In addition, power-frequency and reactive-power-voltage droop control is adopted to obtain proper power sharing without critical communications among DG units, which may have a long distance between each other [2]-[6]. However, the input and output of traditional droop control become fluctuant when an unbalanced impedance is introduced into the microgrid. The power that represents the fundamental negative sequence (FNS) current cannot be proper distributed between DG units under fluctuant load unbalanced state.

A virtual synchronous generator (VSG) balance control method based on negative sequence voltage suppression has been presented in [7]. In [8], [9], a modification of VSG control based on double decoupled synchronous reference frame (DDSRF) decomposition, SG negative-sequence voltage compensation and modified calculation methods for the power and voltage is proposed. They all compensated for the negative sequence voltage. However, their power distribution is not effective.

In [10]-[12], repetitive control is introduced to compensate for voltage unbalance. However, repetitive control always has a delay of about one cycle, which reduces the response rate of

Manuscript received Jan. 27, 2018; accepted Oct. 1, 2018
Recommended for publication by Associate Editor Seon-Ju Ahn.
†Corresponding Author: yaotsin@mail.xjtu.edu.cn
Tel: +86-180-4958-0381, Xi'an Jiaotong University
*Xuji Group Corporation, China
**State Key Laboratory of Electrical Insulation and Power Equipment, Xi'an Jiaotong University, China

the control system. On the other hand, the power distribution problem under the load unbalanced state is not addressed in these articles.

The control method presented in [13] and [14] is based on the feedback of FNS voltage. FNS reactive power Q^- is defined as the product of the FNS voltage and the FNS current. However, the definition of Q^- cannot exactly present the fluctuation of power because the FNS voltage is dramatically suppressed in well-controlled microgrid systems. In addition, the distribution of Q^- is not accurate for using Q^- as the negative feedback factor.

There is a good attempt at improving this control method in [15]. In [15], compensation of voltage unbalance at the PCC is considered. This compensation needs some specific communication lines to send messages from the PCC to each of the DG unit controllers. Thus, the control method makes the system structure more complicated and violates the "Plug & Play" rules [16].

A different definition of FNS reactive power Q^-, which refers to the product of fundamental positive sequence (FPS) voltage and FNS current, is introduced in [17]. Since the effect of the FPS voltage is more significant, this definition is more reasonable. One method for Q^- sharing through the droop control between Q^- and the output admittance has also been proposed. In this method, Q^- is accurately distributed only when the cutoff frequency is in a very high level. However, this is difficult to realize in hardware. Thus, the compensation of unbalance voltage and the accurate distribution of Q^- cannot be achieved at the same time using the control method proposed in [17] and [19].

In this paper, a model of a voltage source inverter is established in the α–β stationary reference frame and the voltage and current controllers are designed. Traditional droop control is illustrated and its inherent problems are pointed out with unbalanced loads in a microgrid. A PR controller is adopted to suppress voltage unbalance. A proportional relationship ($Q^- - Z$ control method) between Q^- and the negative output impedance Z is established to distribute the negative reactive power Q^- accurately and to reduce the effect of unbalanced loads at the same time. Finally, the proposed control strategy is verified by the simulation and experimental results.

This paper is arranged as follows. Sections II describes the model and control of the voltage source inverters. Section III illustrates the traditional droop control and its inherent problems with unbalanced loads in microgrids. Section IV describes the details of the $Q^- - Z$ control method and the whole control structure. Section V and VI show simulation and experimental results to validate the proposed control strategy. Finally, section VII presents some conclusions.

II. Inner Control Design

The whole microgrid structure analyzed in this paper is shown in Fig. 1. It contains two parallel-connected voltage source inverters which represent the DG unit and two static switches to decide whether the inverters are connected to the microgrid. The local and remote loads represent the power demand in the microgrid. The microgrid is operated in the stand-alone mode.

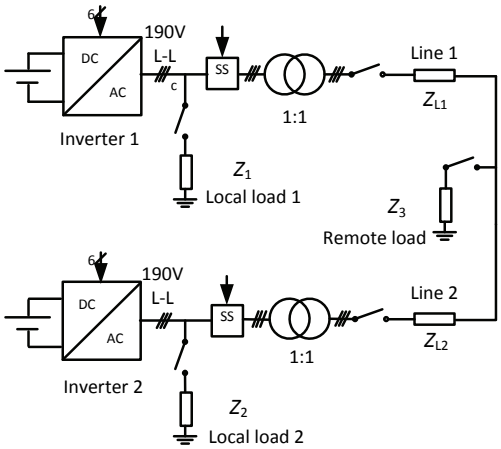

Fig. 1. Microgrid structure.

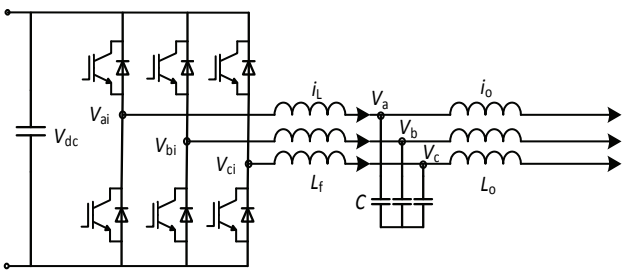

Fig. 2. Voltage source inverter.

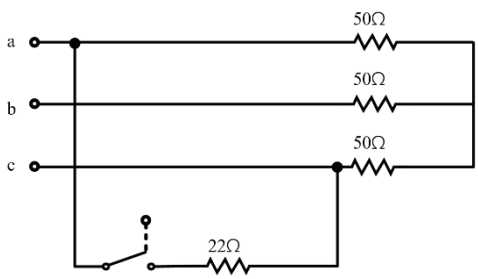

Fig. 3. Three phase unbalanced load circuit.

The voltage source inverter (VSI) chosen as the power electronic interface is shown in Fig. 2. It consists of a three-phase full-bridge inverter and an LC filter. The DC-AC inverter is always controlled as a voltage source, and its control objective is to track the reference voltage value and to suppress disturbances of the load current.

The local and remote loads in the microgrid have the same structures which consist of three phase balanced loads and a 1 phase loads as shown in Fig. 3. A 22Ω resistance is connected between phase A and phase C to imitate the load unbalance state when the switch is closed.

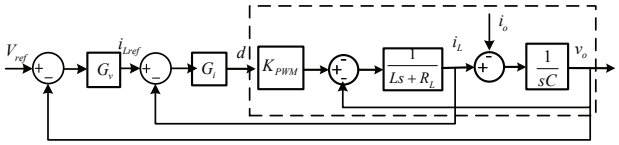

Fig. 4. Control block diagram of a VSI.

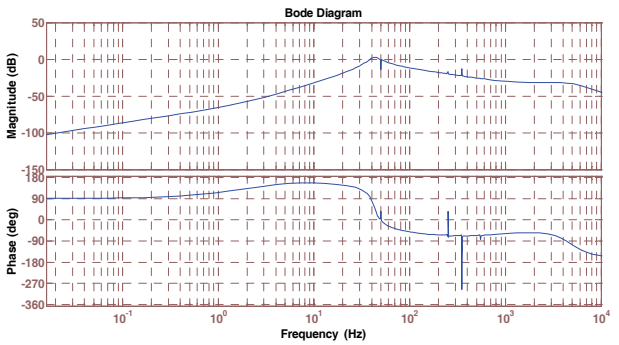

Fig. 5. Bode diagram of the closed voltage loop.

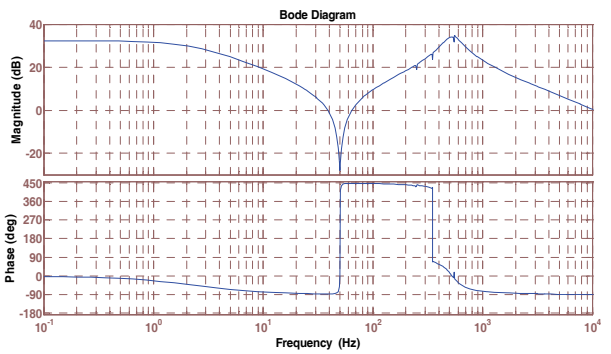

Fig. 6. Bode diagram of the output impedance $Z_0(s)$.

The model and control of the voltage source inverter is in the α–β stationary reference frame, where no coupling exists between the α axis and the β axis. A control block diagram is shown in Fig. 4.

The current controller is:

$$G_i = k \tag{1}$$

where k is the current proportional coefficient. The only goal of the current controller is to increase the system damping.

It is well known that the frequencies of the fundamental frequency of the positive and negative voltages are both 50Hz in the α–β stationary reference frame. For accurate tracking of the voltage reference, a quasi resonant controller is chosen which can provide a very high amplitude at a specified frequency for an open loop Bode diagram. The voltage controller is:

$$G_v = k_{pv} + \frac{2k_v\omega_c s}{s^2 + 2\omega_c s + \omega_0^2} \tag{2}$$

where K_{pv} is the voltage proportional coefficient, K_v is the resonant coefficient, ω_c is the cutoff frequency, and ω_0 is the resonant frequency.

The output voltage in Fig. 4 is:

$$V = G(s)V_{\text{ref}} - Z_{\text{o}}(s)i_{\text{o}} \tag{3}$$

where V_{ref} is the reference voltage, G(s) is the closed-loop transfer function, i_0 is the load current, and Z_0(s) is the output impedance. In addition, G(s) and Z_o(s) are:

$$G(s) = \frac{G_{\text{v}}G_{\text{i}}G_{\text{PWM}}}{LCs^2 + (G_{\text{v}} + Cs)G_{\text{i}}G_{\text{PWM}} + RCs + 1} \tag{4}$$

$$Z_{\text{o}}(s) = \frac{Ls + R + G_{\text{i}}G_{\text{PWM}}}{LCs^2 + (G_{\text{v}} + Cs)G_{\text{i}}G_{\text{PWM}} + RCs + 1} \tag{5}$$

In practice, the design procedure of the PR parameters can be divided into three steps. First, the bandwidth of the controller is determined by the frequency fluctuation range of the power grid so that ω_c is selected. Next, the frequency characteristics of the open-loop transfer function of the controller are selected at the gain of the fundamental frequency K_v. In order to achieve the stability and anti-interference of the system, the K_{pv} parameter is designed based on the harmonic impedance.

The parameters of the voltage and current controllers are then chosen as K_{pv} =0.025, K_v =25, ω_c =4rad/sec, ω_0 =314rad/sec and k=0.1. Then a Bode diagram of the closed loop of the voltage is shown in Fig. 5.

Then a Bode diagram of the output impedance Z_0(s) is shown in Fig. 6.

From Fig. 6 it can be seen that the amplitude of the output impedance at 50Hz is about -30dB. This can effectively suppress the FPS and FNS current disturbances at the fundamental frequency.

III. Traditional Droop Control

The principle of the traditional droop control is to emulate an inverter as a synchronous generator, which decreases the frequency when the output active power increases. The equation of droop control is:

$$f = f_0 - k_{\text{P}}(P - P_0) \tag{6}$$

$$E = E_0 - k_{\text{Q}}(Q - Q_0) \tag{7}$$

where f_0 and E_0 are the nominal frequency and voltage. P_0 and Q_0 are the nominal active and reactive power. P and Q are the instantaneous active and reactive power. f and E are the frequency and voltage reference. Then the droop characteristic is shown in Fig. 7.

Using droop control, the active and reactive power can be shared without critical communications between the inverters. According to the instantaneous reactive power theory, P and

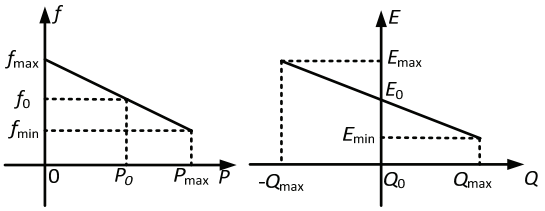

Fig. 7. Droop control characteristic of active and reactive power.

Q are calculated as follows in practical applications:

$$\begin{bmatrix} p \\ q \end{bmatrix} = \begin{bmatrix} v_d & v_q \\ v_q & -v_d \end{bmatrix} \begin{bmatrix} i_d \\ i_q \end{bmatrix} = \begin{bmatrix} v_d i_d + v_q i_q \\ v_q i_d - v_d i_q \end{bmatrix} \tag{8}$$

p and q are constants when there are only linear and balanced loads in a microgrid. However, after loads becoming unbalance, the current contents FPS component and component according to the symmetrical component theory. Thus, in the rotating reference frame the output current becomes:

$$\begin{aligned} i_d &= I_d^+ + I_d^- \cos 2\omega t + I_q^- \sin 2\omega t \\ i_q &= I_q^+ - I_q^- \sin 2\omega t + I_q^- \cos 2\omega t \end{aligned} \tag{9}$$

Substituting the current in (8) with (9), the instantaneous active p and reactive powers q become fluctuant as follows:

$$\begin{aligned} p &= V_d^+ I_d^+ + V_q^+ I_q^+ + (V_d^+ I_d^- + V_q^+ I_q^-)\cos 2\omega t + (V_d^+ I_q^- - V_q^+ I_d^-)\sin 2\omega t \\ q &= V_q^+ I_d^+ - V_d^+ I_q^+ + (V_q^+ I_d^- + V_d^+ I_q^-)\cos 2\omega t + (V_q^+ I_d^- - V_d^+ I_d^-)\sin 2\omega t \end{aligned} \tag{10}$$

Note that the instantaneous active power consists of two parts. The first part is in the DC term, which contains information of the FPS voltage and current. It is as same as the active power of an inverter with balanced loads. The other part is an AC variable at a frequency of 100Hz. The amplitude of the AC variable is calculated as follows:

$$\begin{aligned} Q^- &= \sqrt{(V_d^+ I_d^- + V_q^+ I_q^-)^2 + (V_d^+ I_q^- - V_q^+ I_d^-)^2} \\ &= \sqrt{(V_d^{+2} + V_q^{+2})(I_d^{-2} + I_q^{-2})} = 3V^+ I^- \end{aligned} \tag{11}$$

In [17], the amplitude of the AC variable is called negative reactive power Q^-, because it represents a fluctuation of the active power just like the definition of traditional reactive power. The difference is Q^-, which means the amplitude of the power exchange between the source and the loads. In addition, the traditional reactive power means the amplitude of the power exchange between loads in different phases.

Obviously, the traditional droop control can accurately distribute the DC part in (10). However, it cannot deal with the AC part—negative reactive power Q^-. Thus, the power flow cannot be shared between different DG units in a microgrid with unbalanced loads by only using traditional droop control. A Q^- distribution method is needed to solve this problem.

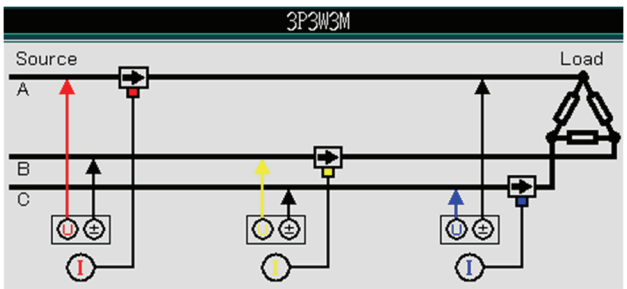

Fig. 8. Probe connection diagram for Q^- calculation.

One point should be mentioned is that the FNS reactive power Q^- can be calculated with 3-phase traditional active power. The only requirement is a power analyzer that has 3 voltage probes, 3 current probes and is connected as shown in Fig. 8.

Traditional 3-phase active power is calculated as follows, where U_p is the voltage peak value, I_p^+ is the peak value of the FPS current, and I_p^- is the peak value of the FNS current.

$$\begin{aligned} P_1 &= \frac{1}{2\pi}\int_0^{2\pi}\{U_p\cos\theta_1[I_p^+\cos(\theta_1+\Phi^+)+I_p^-\cos(\theta_1+\Phi^-)]\}d\theta_1 \\ P_2 &= \frac{1}{2\pi}\int_0^{2\pi}\{U_p\cos\theta_2[I_p^+\cos(\theta_2+\Phi^+)+I_p^-\cos(\theta_2+\Phi^-+\frac{2\pi}{3})]\}d\theta_2 \\ P_3 &= \frac{1}{2\pi}\int_0^{2\pi}\{U_p\cos\theta_3[I_p^+\cos(\theta_3+\Phi^+)+I_p^-\cos(\theta_3+\Phi^-+\frac{2\pi}{3})]\}d\theta_3 \end{aligned} \tag{12}$$

Calculating the integral term yields:

$$\begin{aligned} P_1 &= \frac{1}{2\pi}\int_0^{2\pi}\{U_p\cos\theta_1[I_p^+\cos(\theta_1+\Phi^+)+I_p^-\cos(\theta_1+\Phi^-)]\}d\theta_1 \\ P_2 &= \frac{1}{2\pi}\int_0^{2\pi}\{U_p\cos\theta_2[I_p^+\cos(\theta_2+\Phi^+)+I_p^-\cos(\theta_2+\Phi^-+\frac{2\pi}{3})]\}d\theta_2 \\ P_3 &= \frac{1}{2\pi}\int_0^{2\pi}\{U_p\cos\theta_3[I_p^+\cos(\theta_3+\Phi^+)+I_p^-\cos(\theta_3+\Phi^-+\frac{2\pi}{3})]\}d\theta_3 \end{aligned} \tag{13}$$

In practice, P_1, P_2 and P_3 can be measured with a power analyzer and all of them should be multiplied by $2/\sqrt{3}$ to get the accurate sum of all three phases. Thus, (13) can be seen as a ternary equation. Treating $U_p I_p^-$ as an unknown and solving the ternary equation yields:

$$Q^- = \sqrt{3}U_p I_p^- = \frac{4}{\sqrt{3}}\sqrt{P_1^2 + P_2^2 + P_3^2 - P_1P_2 - P_2P_3 - P_1P_3} \tag{14}$$

(14) proves that Q^- means the amplitude of the power exchange between the source and the loads from the angle of the traditional power definition. In addition, (14) can be used in practice to calculate Q^- with a power analyzer.

IV. Q-Z Control

A. $Q^- - Z$ Control

In a well-controlled microgrid, the FPS voltage V^+ can usually be seen as a constant. Thus, sharing an accurate Q^-

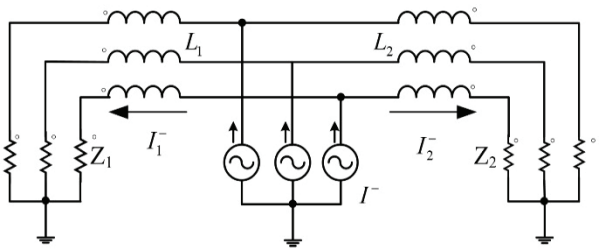

Fig. 9. Equivalent circuit of the FNS current sharing of a DG unit.

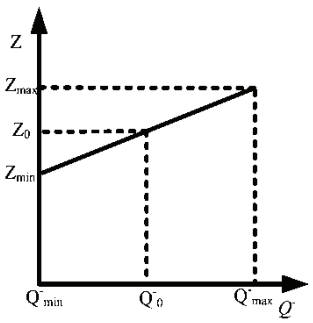

Fig. 10. $Q^- - Z$ control characteristic.

means an accurate distribution of the FNS output current I-. Considering a microgrid that consists of two DG units and one 3 phase unbalanced load, the DG unit keeps the output voltage very well at a fundamental frequency sinewave without unbalance or harmonic. Then the FNS current is brought in when the fundamental frequency voltage acts on unbalanced loads. When only the FNS current is considered, the unbalanced loads can be substituted with FNS current sources as below.

In Fig. 9, Z_1, Z_2 refers to the output impedance of a DG unit. Obviously, the FNS current can be shared accurately if Z_1, Z_2 can be controlled in proportion. Thus, a proportional relationship is built to operate output impedance of each DG unit.

$$Z = Z_0 + \mu_Z(Q^- - Q_0^-) \tag{15}$$

As shown in Fig. 10, if outputs Q^- of one of the DG units increases, the $Q^- - Z$ control orders the DG unit to increase its output impedance to decrease the FNS output current I^-. This in turn, achieves the goal of compensating the increased Q^-.

The $Q^- - Z$ control can also be shown to be effective in math. In (11), substitute I^- with (15):

$$Q^- = 3V^+I^- = \frac{3V^+V^-}{Z} = \frac{3V^+V^-}{Z_0 + \mu_Z(Q^- - Q_0^-)} \tag{16}$$

(16) can be simplified as follows:

$$\mu_Z(Q^-)^2 + (Z_0 - \mu_Z Q_0^-)Q^- - 3V^+V^- = 0 \tag{17}$$

Solving this equation yields:

$$Q^- = \frac{\mu_Z Q_0^- - Z_0 + \sqrt{(\mu_Z Q_0^- - Z_0)^2 + 12\mu_Z V^+V^-}}{2\mu_Z} \tag{18}$$

If the following conditions are met:

$$(\mu_Z Q_0^- - Z_0)^2 >> 12\mu_Z V^+V^- \tag{19}$$

(18) can be simplified as follows:

$$Q^- = \frac{\mu_Z Q_0^- - Z_0}{\mu_Z} \tag{20}$$

Thus, assume that the $Q^- - Z$ control coefficients of two DG units are assigned according to the following relationship:

$$\begin{aligned} &\frac{Q_{01}^-}{Q_{02}^-} = \frac{\mu_{Z2}}{\mu_{Z1}} \\ &Z_{01} = Z_{02} \end{aligned} \tag{21}$$

Substitute (21) into (20). Then:

$$\frac{Q_1^-}{Q_2^-} = \frac{\mu_{Z1}Q_{01}^- - Z_{01}}{\mu_{Z2}Q_{02}^- - Z_{02}} \cdot \frac{\mu_{Z2}}{\mu_{Z1}} = \frac{\mu_{Z2}}{\mu_{Z1}} = \frac{Q_{01}^-}{Q_{02}^-} \tag{22}$$

When the relationship of formula (19) is satisfied, the simplified formula (20) can be obtained. The formula (21) is a hypothetical relationship. Through a combination of formula (21) and formula (20), formula (22) can be obtained. Then the two inverters automatically assign their respective negative-sequence reactive power according to the set ratio.

Obviously, two DG units can share Q^- in proportion to their rated capacity.

The same principle can be applied for a microgrid with multiple installations of DG units. By assigning the droop coefficients of various DG units as (23), each of the DG units can share Q^- in proportion to their rated capacity.

$$\begin{aligned} &Q_{01}^-\mu_{Z1} = Q_{02}^-\mu_{Z2} = \cdots = Q_{0N}^-\mu_{ZN} \\ &Z_{01} = Z_{02} = \cdots = Z_{0N} \end{aligned} \tag{23}$$

Each DG unit can share Q^- in proportion to their rated capacity.

B. DG Unit Control System with $Q^- - Z$ Control

The DG unit control system with $Q^- - Z$ control is shown in Fig. 11.

First, sequence separation is used to separate the output voltage and current into FPS and FNS. P and Q are calculated with the FPS voltage and current. Then, they are transmitted into a traditional droop controller which gives the FPS voltage reference to accurately share the active and reactive power. Q^- is calculated using the FPS voltage and FNS current. The $Q^- - Z$ controller gives the FNS output impedance to accurately distribute the FNS reactive power Q^-. Then, the FNS voltage reference is calculated as the product of Z and the FNS output current. Finally, V_{ref} which

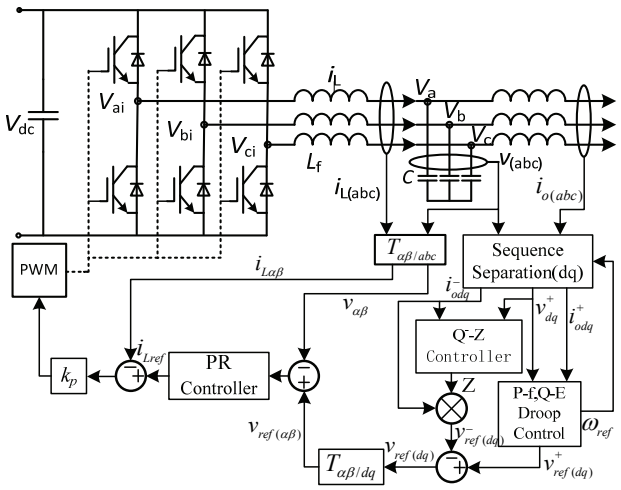

Fig. 11. DG unit control diagram with $Q^- - Z$ control.

means the sum of the FPS voltage reference and the FNS voltage reference is used as the reference of the voltage control loop and the PR controller ensure the quality of the DG unit's output voltage.

The increase of the negative sequence impedance of the system leads to an increase of the voltage unbalance factor (VUF). In order to keep the VUF from exceeding 3%, this paper limits the output impedance Z by 0-3Ω.

V. Simulation Results

A. Simulation with Two DG Units

In order to verify the proposed control strategy, a simulation is implemented in PSIM, and the simulation circuit is shown in Fig. 12. Two inverters are connected in parallel and the switching frequency is 10 kHz. The rated active and reactive powers of the inverters are both 4kW and 3kVar, the nominal power is P_0=2kW, Q_0=0kVar, and the droop coefficients are k_P =0.1Hz/kW and k_Q =4.43V/kVar. The only difference is the line impedance between the two inverters, one is 3mH and the other is 2mH.

Results of the traditional droop control with unbalanced loads are shown in Fig. 13. It can be seen that the active and reactive powers are both fluctuant for the FNS current. In addition, the amplitude of the power fluctuation is equal to the FNS reactive power Q^- as derived previously.

Using the $Q^- - Z$ control to deal with the FNS reactive power Q^-, the $Q^- - Z$ control coefficients are set as follows:

$$Z = 1 + (Q^- - 800) \times 2.5 \times 10^{-3} \tag{24}$$

Results of the $Q^- - Z$ control with different line impedances (3mH and 2mH) are shown in Fig.14. Neglecting the difference of the line impedance, the FNS reactive power of the two inverters are distributed at a ratio of 1:1.05. In addition, their active and reactive power are also well shared

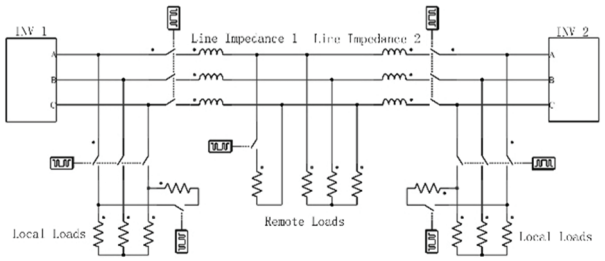

Fig. 12. PSIM simulation circuit.

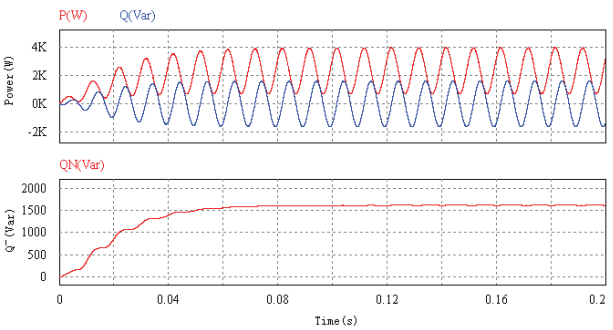

Fig. 13. Instantaneous power in a microgrid with unbalanced loads.

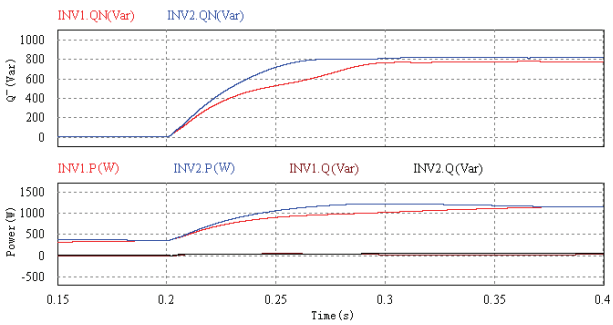

Fig. 14. Power distribution results using the $Q^- - Z$ control.

by using the traditional droop control.

The voltage unbalance factor (VUF) and an output voltage waveform of inverter 2 are shown in Fig. 14. The VUF is calculated as follows:

$$VUF = \frac{v^-_{rms}}{v^+_{rms}} \times 100\% \tag{25}$$

It can be seen that in Fig. 15, the VUFs of the two inverters are both less than 2%, which indicates that the DG unit' output voltage unbalance is well compensated with the $Q^- - Z$ control. The VUF is suggested to be less than 3% according to IEEE1547 standard [18].

The target ratio of the two inverter sharing is set to 1.5:1 and the line impedances are both 3mH. The $Q^- - Z$ control coefficients are set as:

$$\begin{aligned} Z_1 &= 1 + (Q^- - 900) \times 2 \times 10^{-3} \\ Z_2 &= 1 + (Q^- - 600) \times 3 \times 10^{-3} \end{aligned} \tag{26}$$

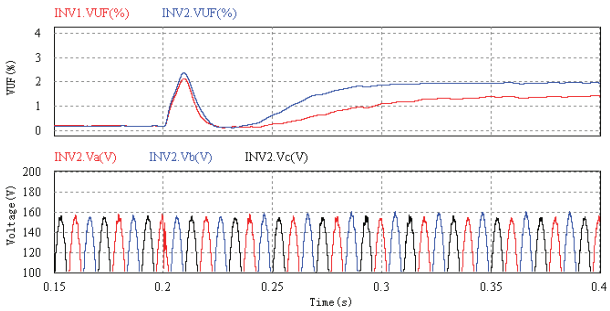

Fig. 15. VUF and voltage waveform using the $Q^{-}-Z$ control.

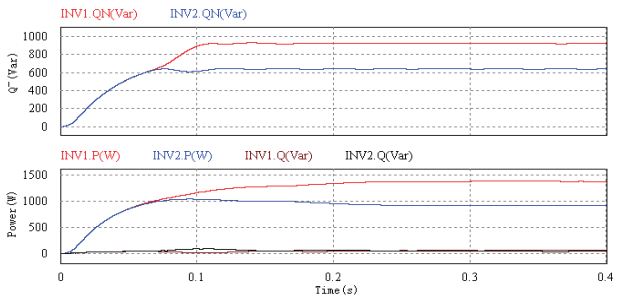

Fig. 16. Power sharing result when the rated capacity proportion is 1.5:1.

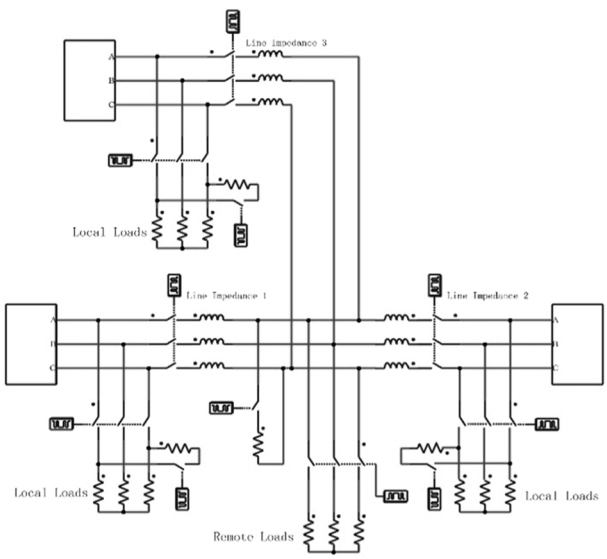

Fig. 17. PSIM simulation circuit.

The power sharing result is shown in Fig. 16.

Obviously, the Q^{-} distribution result is 1.45:1, which is an accurate tracking of the target ratio. Fig. 16 also shows that the $Q^{-}-Z$ control does not disturb the traditional droop control which is effective for the P and Q distribution.

B. Simulation with Three DG Units

In order to achieve generality with the proposed method, the simulation study of the system is implemented with 3 DG units. The simulation is implemented in PSIM, and the simulation circuit is shown in Fig. 17. The line impedances between the three inverters are 4mH, 3mH and 2mH respectively.

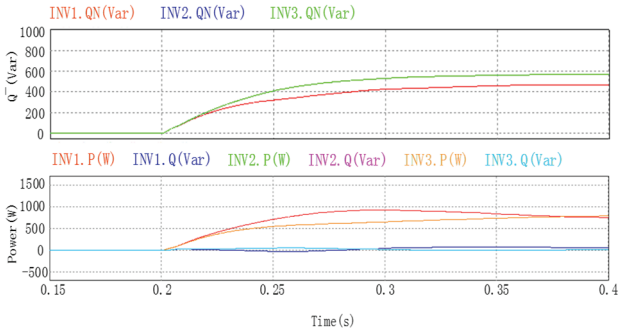

Fig. 18. Power distribution results using the $Q^{-}-Z$ control.

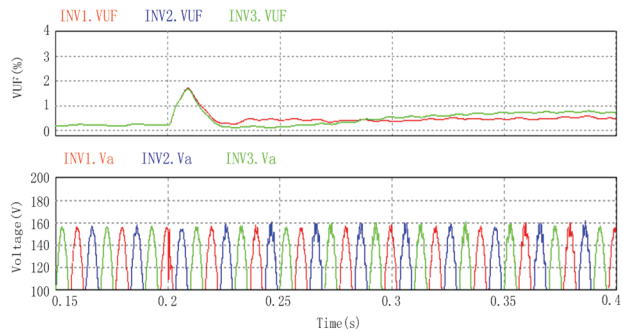

Fig. 19. VUF and voltage a waveform using the $Q^{-}-Z$ control.

As shown in Fig. 18, the ratio of the FNS reactive power of the three inverters is 1:1:1.05. This shows that the proposed method can reduce the influence of the line impedance on the reactive power distribution of the line and that it is compatible with the traditional droop control. In addition, the active and reactive power are well shared by using the traditional droop control.

This also shows that in Fig. 19, the VUF of the three inverters are both less than 2%. According to IEEE1547 standard [18], the VUF should be less than 3%. These results show that the DG unit' output voltage unbalance is well compensated with the $Q^{-}-Z$ control.

VI. Experimental Results

The experimental setup is shown in Fig. 20. It contains two parallel inverters, a static switch, line impedances and unbalanced loads. A digital processor TMS320F28335 is used to deal with the control algorithms.

The results of the $Q^{-}-Z$ control with the same DG unit' capacity and different line impedances (2mH and 3mH) are shown in Fig. 21 and Fig. 22. Q_1^{-} and Q_2^{-}, which can be calculated using (14), are 855.1Var and 787.7Var, respectively. $Q_1^{-}:Q_2^{-}$ = 1.08:1, it is close to the goal of same capacity. This also shows that the traditional power P and Q is shared well at the same time.

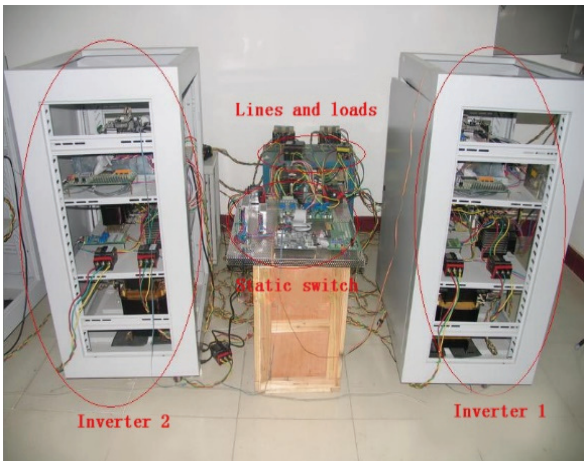

Fig. 20. Experimental setup.

Urms1	182.08	V	S1	0.715k	VA
Urms2	188.98	V	S2	0.408k	VA
Urms3	182.22	V	S3	0.381k	VA
Urms123	184.43	V	S123	1.504k	VA
Irms1	6.885	A	Q1	0.037k	var
Irms2	3.792	A	Q2	0.295k	var
Irms3	3.533	A	Q3	-0.246k	var
Irms123	4.736	A	Q123	0.087k	var
P1	0.714k	W	φ1	2.98	°
P2	0.282k	W	φ2	46.35	°
P3	0.291k	W	φ3	-40.13	°
P123	1.287k	W	φ123	31.17	°
λ1	0.9986		f1	50.069	Hz
λ2	0.6903		f2	50.074	Hz
λ3	-0.7646		f3	50.076	Hz
λ123	0.8556				

Fig. 21. Power of Inverter1 with different line impedances.

Urms1	183.60	V	S1	0.714k	VA
Urms2	190.07	V	S2	0.428k	VA
Urms3	185.59	V	S3	0.388k	VA
Urms123	186.42	V	S123	1.530k	VA
Irms1	6.767	A	Q1	0.176k	var
Irms2	3.962	A	Q2	0.343k	var
Irms3	3.549	A	Q3	-0.139k	var
Irms123	4.758	A	Q123	0.380k	var
P1	0.692k	W	φ1	14.30	°
P2	0.256k	W	φ2	53.30	°
P3	0.362k	W	φ3	-21.02	°
P123	1.310k	W	φ123	31.11	°
λ1	0.8830		f1	50.068	Hz
λ2	0.5977		f2	50.062	Hz
λ3	-0.9335		f3	50.075	Hz
λ123	0.8561				

Fig. 22. Power of Inverter2 with different line impedances.

Urms1	182.08	V	Upk1+	264.81	V
Urms2	188.98	V	Upk2+	257.63	V
Urms3	182.22	V	Upk3+	259.64	V
Urms123	184.43	V	Upk1-	-266.95	V
Umn1	180.44	V	Upk2-	-259.45	V
Umn2	190.44	V	Upk3-	-259.12	V
Umn3	182.25	V	Udc1	0.00	V
Umn123	184.38	V	Udc2	0.00	V
Ufnd1	182.01	V	Udc3	0.00	V
Ufnd2	188.78	V	Uac1	182.08	V
Ufnd3	182.28	V	Uac2	188.98	V
Uthd1	3.04	%	Uac3	182.22	V
Uthd2	4.28	%	f1	50.069	Hz
Uthd3	2.56	%	f2	50.074	Hz
Uunb	2.42	%	f3	50.076	Hz

Fig. 23. Maximum VUF with different line impedances.

Urms1	187.05	V	S1	0.793k	VA
Urms2	189.69	V	S2	0.438k	VA
Urms3	186.60	V	S3	0.446k	VA
Urms123	187.78	V	S123	1.677k	VA
Irms1	7.393	A	Q1	0.145k	var
Irms2	4.012	A	Q2	0.325k	var
Irms3	4.096	A	Q3	-0.208k	var
Irms123	5.167	A	Q123	0.262k	var
P1	0.780k	W	φ1	10.52	°
P2	0.293k	W	φ2	47.96	°
P3	0.394k	W	φ3	-27.79	°
P123	1.468k	W	φ123	28.93	°
λ1	0.9832		f1	50.102	Hz
λ2	0.6697		f2	50.111	Hz
λ3	-0.8847		f3	50.106	Hz
λ123	0.8752				

Fig. 24. Power of inverter1 for a 1.5:1 distribution target ratio.

Urms1	182.95	V	S1	0.543k	VA
Urms2	189.65	V	S2	0.364k	VA
Urms3	184.42	V	S3	0.248k	VA
Urms123	185.68	V	S123	1.156k	VA
Irms1	5.123	A	Q1	0.057k	var
Irms2	3.356	A	Q2	0.276k	var
Irms3	2.273	A	Q3	-0.119k	var
Irms123	3.584	A	Q123	0.213k	var
P1	0.540k	W	φ1	5.98	°
P2	0.238k	W	φ2	49.21	°
P3	0.218k	W	φ3	-28.68	°
P123	0.996k	W	φ123	30.48	°
λ1	0.9946		f1	50.096	Hz
λ2	0.6533		f2	50.103	Hz
λ3	-0.8774		f3	50.109	Hz
λ123	0.8618				

Fig. 25. Power of inverter2 for a 1.5:1 distribution target ratio.

Urms1	182.95	V	Upk1+	265.19	V
Urms2	189.65	V	Upk2+	261.04	V
Urms3	184.42	V	Upk3+	262.24	V
Urms123	185.68	V	Upk1-	-270.23	V
Umn1	181.01	V	Upk2-	-259.97	V
Umn2	191.16	V	Upk3-	-261.53	V
Umn3	184.21	V	Udc1	0.00	V
Umn123	185.46	V	Udc2	0.00	V
Ufnd1	182.64	V	Udc3	0.00	V
Ufnd2	189.38	V	Uac1	182.95	V
Ufnd3	184.37	V	Uac2	189.65	V
Uthd1	3.34	%	Uac3	184.42	V
Uthd2	4.50	%	f1	50.113	Hz
Uthd3	2.26	%	f2	50.099	Hz
Uunb	2.79	%	f3	50.100	Hz

Fig. 26. Maximum VUF for a 1.5:1 distribution target ratio.

The voltage unbalance factor can be seen in Fig. 23. Only the voltage situation of invereter1 is shown since its VUF is larger than the VUF of inverter2. The VUF of inverter1 represents the maximum VUF in the microgrid. Fig. 20 indicates that the $Q^- - Z$ control decreases the VUF at 2.42%, which is less than the IEEE1546 suggestion of 3%.

The results of the $Q^- - Z$ control with a target sharing ratio of 1.5:1 and the same 3mH line impedances are shown in Fig. 24 and Fig. 25. Using (14), it can be easily calculated that Q_1^- =890.4Var and Q_2^- =625.0Var. Therefore, $Q_1^- : Q_2^-$ =1.42:1 which meets the target ratio of 1.5:1 very well. On the other hand, the proportional ratio of P and Q of the two inverters also is close to the distribution target.

TABLE I
EXPERIMENT RESULT SUMMARY OF THE $Q^- - Z$ CONTROL

Target ratio	Q_1^- (Var)	Q_2^- (Var)	$Q_1^- : Q_2^-$	Max VUF
1:1	855.1	787.7	1.08:1	2.42%
1.5:1	890.4	625.0	1.42:1	2.79%

Fig. 26 shows the voltage result of a 1.5:1 distribution target ratio when the $Q^- - Z$ control is used. The maximum VUF is 2.79%, which is less than the IEEE1546 suggestion of 3%.

Table I summarizes the experimental results of a microgrid using the $Q^- - Z$ control. Obviously, the $Q^- - Z$ control can share Q^- accurately according to the target ratio and suppress the VUF in the microgrid at the same time. One point that should be mentioned is that the increase of the maximum VUF in the microgrid is caused by the different values of Q^- for the two DG units. According to the different $Q^- - Z$ control, a larger Q^- lead to a larger Z. In addition, a larger output impedance means that the output voltage is more easily influenced by an unbalanced output current. Thus, the maximum VUF of the target ratio of 1.5:1 is larger.

VII. CONCLUSIONS

In this paper, a model of a voltage source inverter is established in the α–β stationary reference frame and voltage and current controllers are designed. The traditional droop control is illustrated and its inherent problems are pointed out when unbalanced loads are introduced into a microgrid. Since the traditional droop control cannot share Q^-, the $Q^- - Z$ droop control is introduced as a supplement to the old power sharing method. By using the $Q^- - Z$ droop control to distribute the negative sequence reactive power Q^-, the unbalanced current in a microgrid can be reasonably configured. So that it will not affect the stability of a system, the proposed method can maintain the VUF at a low level while effectively distributing Q^-. Thus, together with the traditional droop control algorithm, a complete power distribution system is proposed.

REFERENCES

[1] F. Katiraei, R. Iravani, N. Hatziargyriou, and A. Dimeas, "Microgrids management," *IEEE Power Energy Mag.*, Vol. 6, No. 3, pp. 54-65, May/Jun. 2008.

[2] L. Yunwei, D. M. Vilathgamuwa, and P. C. Loh, "Design, analysis, and real-time testing of a controller for multibus microgrid system," *IEEE Trans. Power Electron.*, Vol. 19, No. 5, pp. 1195-1204, Sep. 2004.

[3] J. M. Guerrero, J. C. Vasquez, J. Matas, L. G. D. Vicuna, and M. Castilla, "Hierarchical control of droop-controlled AC and DC microgrids – A general approach toward standardization," *IEEE Trans. Ind. Electron.*, Vol. 58, No. 1, pp. 158-172, Jan. 2011.

[4] J. M. Guerrero, J. C. Vasquez, J. Matas, M. Castilla, and L. G. D. Vicuna, "Control strategy for flexible microgrid based on parallel line-interactive UPS systems," *IEEE Trans. Ind. Electron*., Vol. 56, No. 3, pp. 726-736, Mar. 2009.

[5] J. M. Guerrero, J. Matas, L. G. D. Vicuna, M. Castilla, and J. Miret, "Decentralized control for parallel operation of distributed generation inverters using resistive output impedance," *IEEE Trans. Ind. Electron.*, Vol. 54, pp. 994-1004, 2007.

[6] K. De Brabandere, B. Bolsens, D. K. J. Van, A. Woyte, J. Driesen, and R. Belmans, "A voltage and frequency droop control method for parallel inverters," *IEEE Trans. Power Electron.*, Vol. 22, No. 4, pp. 1107-1115, Jul. 2007.

[7] T. Chen, L. Chen, Y. Wang, T. Zhen, and S. Mei, "Balanced current control of virtual synchronous generator considering unbalanced grid voltage," *Power System Technology*, Vol. 40, No. 3, pp. 904-909, 2016. (in Chinese)

[8] J. Liu, M. Yushi, T. Ise, Y. Jin, and K. Watanabe, "Parallel operation of a synchronous generator and a virtual synchronous generator under unbalanced loading condition in microgrids," *IEEE 8th International Power Electronics and Motion Control Conference (IPEMC-ECCE Asia)*, pp. 3741-3748, 2016.

[9] Q. Liu, T. Yong, L. Xunhao, Y. Deng, and X. He, "Voltage unbalance and harmonics compensation for islanded microgrid inverters," *IET Power Electron.*, Vol. 7, No. 5, pp. 1055-1063, May 2014.

[10] M. B. Delghavi and A. Yazdani, "Islanded-mode control of electronically coupled distributed-resource units under unbalanced and nonlinear load conditions," *IEEE Trans. Power Del.*, Vol. 26, No. 1, pp. 661-673, Apr. 2011.

[11] T. Hornik and Q. Zhong, "H∞ repetitive current-voltage control of inverters in microgrids," *IECON 36th Annual Conference on IEEE Industrial Electronics Society*, pp. 3000-3005, 2010.

[12] T. Hornik and Q. Zhong, "A current-control strategy for voltage-source inverters in microgrids based on and repetitive control," *IEEE Trans. Power Electron.*, Vol. 26, No. 3, pp. 943-952, Mar. 2011.

[13] M. Savaghebi, J. M. Guerrero, A. Jalilian, and J. C. Vasquez, "Experimental evaluation of voltage unbalance compensation in an islanded microgrid," *IEEE International Symposium on Industrial Electronics (ISIE 2011)*, pp. 1453-1458, 2011.

[14] M. Savaghebi, A. Jalilian, and J. C. Vasquez, "Autonomous Voltage unbalance compensation in an islanded droop-controlled microgrid," *IEEE Trans. Ind. Electron.*, Vol. 60, No. 4, pp. 1390-1402, Apr. 2013.

[15] M. Savaghebi, J. M. Guerrero, and A. Jalilian, "Secondary control for voltage unbalance compensation in an islanded microgrid," *IEEE International Conference on Smart Grid Communications (Smart Grid Comm)*, pp. 499-504, 2011.

[16] R. H. Lasseter, J. H. Eto, B. Schenkman, J. Stevens, H. Vollkommer, and D. Klaap, "CERTS microgrid laboratory test bed," *IEEE Trans. Power Del.*, Vol. 26, No. 1, pp. 325-332, Jan. 2011.

[17] P. T. Cheng, C. Chen, T. L. Lee, and S. Y. Kuo, "A cooperative imbalance compensation method for distributed generation interface converters," *IEEE Trans. Ind. Appl*., Vol. 45, No. 2, pp. 805-815, Mar./Apr. 2009.
[18] IEEE Application Guide for IEEE Std 1547(TM), IEEE Standard for Interconnecting Distributed Resources with Electric Power Systems, IEEE Std 1547.2-2008, 2009.
[19] X. Zhao, X. Wu, L. Meng, J. M. Guerrero, and J. C. Vasquez, "A direct voltage unbalance compensation strategy for islanded microgrids," I*EEE Applied Power Electronics Conference and Exposition (APEC)*, pp. 3252-3259, 2015.

Yaoqin Jia received his B.S. degree in Electrical Engineering from Beihang University, Beijing, China; and his M.S. and Ph.D. degrees from Xi'an Jiaotong University (XJTU), Xi'an, China, in 1998 and 2003, respectively. He studied at the Tokyo Institute of Technology, Tokyo, Japan, in 2000. He worked in a factory for three years. He worked as a Post-Doctoral Fellow at Tsinghua University, Beijing, China, in 2003. He is presently working as an Associate Professor in the Department of Electrical Engineering, XJTU. His current research interests include digital control in power electronics and distributed power systems.

Daoyang Li was born in Xi'an, China. He received his B.S. and M.S. degrees in Electrical Engineering from Xi'an Jiaotong University (XJTU), Xi'an, China, in 2010 and 2013, respectively, where he conducted research on the control of inverters in microgrids. He is presently working as an Engineer at Xuji Group Corporation, Xuchang, China. His current research interests include flexible HVDC technologies.

Zhen Chen received his B.S. degree in Electrical Engineering from Nan Chang University (NCU), Jiangxi, China. He is presently working towards his M.S. degree at Xi'an Jiaotong University (XJTU), Xi'an, China. His current research interests include microgrids and digital control in power electronics.